Photochemical &
Photobiological Sciences

https://doi.org/10.1039/C9PP00243J

Recovery of photodegraded rhodamine 6g in ester-containing polymer matrices

Nicholas D. Christianson,[a] Yunli Lu,[a] and Nathan J. Dawson*[a,b,c]

Author prepared
post-print of Photochem.
Photobiol. Sci., 18,
2865-2874 (2019)

DOI: 10.1039/C9PP00243J

Self-healing, rhodamine 6g, dye-doped polymers are reported. The amplified spontaneous emission (ASE) photodegrades after repeated exposure to 532 nm laser light at 10 Hz. Recovery of the ASE signal is observed in dye-doped thermoplastic polyurethane and glycol-modified poly(ethylene terephthalate); both polymers contain repeating ester groups in their backbone. The polymer ester groups are hypothesized to mediate the full recovery of rhodamine 6g from a photodegraded state. A small amount of ASE recovery after photodegradation is observed in dye-doped poly(vinyl alcohol), $>98\%$ hydrolyzed, where conversion of rhodamine 6g from a long-lived dark state contributes to the majority of the increased ASE signal in poly(vinyl alcohol) while small amounts of recovery from interactions with residual acetate groups are also possible.

1 Introduction

Organic molecules are used in many optical materials for colorants,[1] photovoltaics,[2,3] nonlinear optics,[4,5] and fluorescent markers.[6,7] The low cost and tailorable optical properties of organic molecules makes them useful for device applications. The operational lifetime of an optical material subject to high intensities is determined by the materials' intensity-dependent photodegradation,[8,9] which currently limits the use of organic optical materials in many device classes. Researchers have worked to uncover some aspects of photodegradation in specific molecular systems;[10,11] however, the current understanding of photodegradation, broadly defined, is still limited. The large assortment of molecular configurations and local environments result in many possible photodegradation pathways, where no simple generalized theory of photodegradation can be established. Mechanisms of photodegradation can include phototautomerization,[12] photodenaturation,[13] photoejection,[14] triplet-radical reactions,[15] photodissociation,[16] and intramolecular charge transfer,[17] to name a few. The self-healing phenomenon observed in some dye-doped systems[18] could be used to create long-lifetime, optical devices. The reversibility of some photo-processes are well-known such as the UV-induced photoisomerization and thermal relaxation of azobenzene derivatives;[19] however, some systems can have more complex behaviors. There are only a limited number of known dye-host systems that undergo photobleaching followed by either partial or full recovery in the dark.

Recovery of an organic dye-doped polymer's fluorescence was first reported in a study by Peng *et al.*, which included rhodamine B, fluorescein, and pyrromethene dyes in a poly(methylmethacrylate) (PMMA) matrix.[20] The anthraquinone dye, disperse orange 11 (DO11), was later placed in a PMMA host to create a self-healing material that fully recovers after being severely degraded by a pump beam.[21] Perylene di-imide derivatives dispersed in PMMA were observed to undergo partial recovery in the presence of oxygen with no recovery observed in anaerobic conditions, which evidences competing reversible and irreversible photodegradation pathways.[22] Since its self-healing properties were discovered, many studies have been performed on DO11-doped PMMA to determine the recovery rate's dependencies on environmental conditions. Such studies have investigated the recovery rate's dependence on external electric fields,[23,24] temperature,[25,26] concentration,[27] and the excitation wavelength.[28] The transient recovery of DO11-doped PMMA has also been studied in thick samples where pump depletion occurs through the sample.[29] The photodegradation and recovery of DO11-doped PMMA has also been studied locally over the cross-section of a photobleached region.[30] The hypothesis for one specific polymer mediated self-healing process, in which the dye's recovery is specific to the polymer, was strongly supported by studying DO11-doped PMMA/polystyrene copolymers;[31] the recovery of DO11 decreased as the weight percentage of PS increased in a PMMA/PS copolymer host. Other classes of molecules have also been shown to recover in PMMA, namely the two-photon fluorescence recovery of the molecule AF455 when doped in PMMA.[32] Self-healing materials can be used to create self-healing optical and electro-optical devices, where modern light-responsive de-

[a] Department of Natural Sciences, Hawaii Pacific University, Kaneohe, USA
[b] Department of Computer Science and Engineering, Hawaii Pacific University, Honolulu, USA
[c] Department of Physics and Astronomy, Washington State University, Pullman, USA
* E-mail: ndawson@hpu.edu

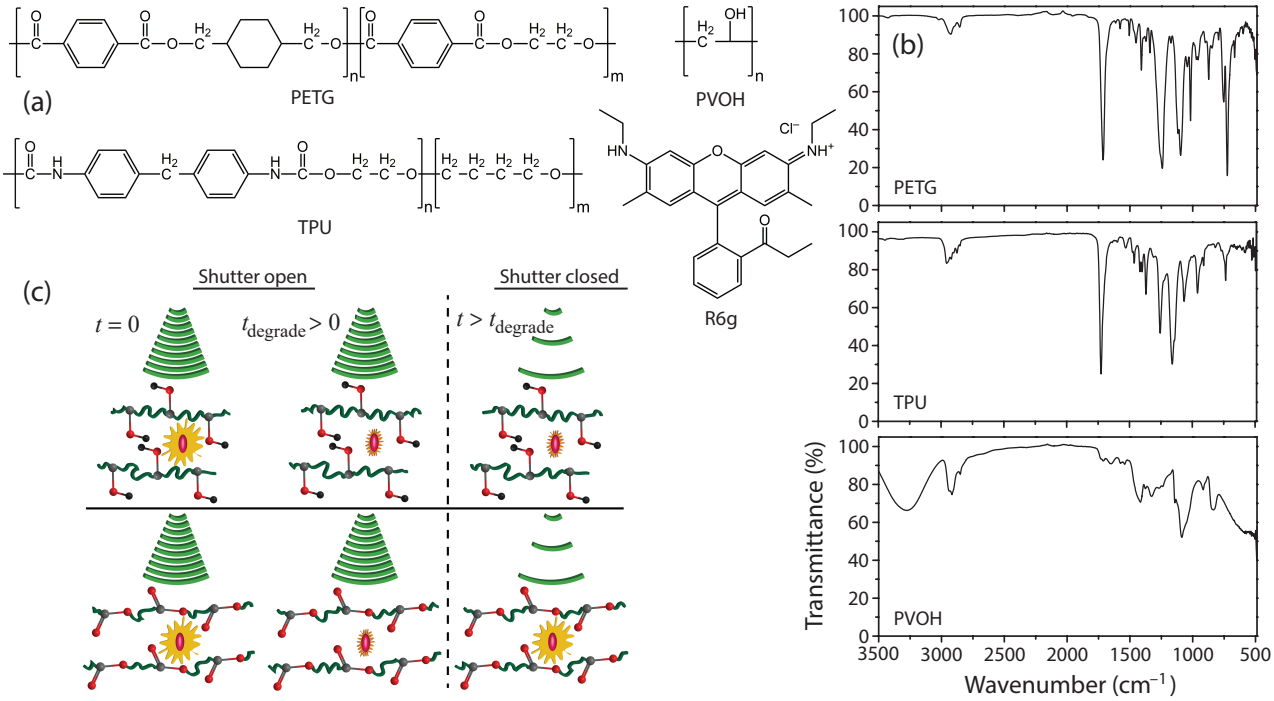

Fig. 1 (a) The chemical structures for Rhodamine 6g (R6g) perchlorate and the polymer matrices glycol-modified poly(ethylene terephthalate) (PETG), thermoplastic polyurethane (TPU), and poly(vinyl alcohol) (PVOH). (b) FTIR spectra for *undoped* PETG, TPU, and PVOH films. (c) An strobed illustration of the self-healing experiments in which R6g-doped polymers are illuminated with a pulse laser. Chromophores initially ($t = 0$) emit radiation after light absorption until they eventually photodegrade ($t = t_{\text{degrade}}$). The material is left in the dark and infrequently probed with the laser source. Photodegraded R6g molecules doped in polymers with repeating ester groups recover their fluorescence while those doped in the polymer without ester groups do not recover.

vices have been observed to self-heal after being photodegraded by visible light such as electroluminescent devices[33] and perovskite photovoltaic devices.[34]

The self-healing phenomena of DO11-doped PMMA has been extensively studied since its discovery. Either partial or complete healing for a large assortment of anthraquinone dyes have been reported in PMMA.[35] PMMA was the only host polymer known to promote the healing of photodegraded chromophores until 2015 when Anderson *et al.* showed that a partially photobleached random laser with rhodamine 6g (R6g) dispersed in polyurethane recovered after partial photobleaching.[36,37] A similar random laser fabricated with a DO11-doped PMMA gain medium resulted in similar self-healing behavior.[38] A third polymer host that promotes self-healing of DO11 was discovered in 2018 by Stubbs *et al.*,[39] where the amplified spontaneous emission (ASE) of a DO11-doped polylactic acid (PLA) polymer was shown to fully recovery. Each of these polymers has repeating ester functional groups either in the polymer backbone or as part of the side-chain. Thus, we expect other ester containing polymers to also promote the recovery of specific photodegraded dyes. In this paper, we observe the periodically probed ASE intensity after partial photodegradation of R6g in three polymers. The results inductively add further evidence to support the ester hypothesis of self-healing, dye-doped polymers in which an intermediate interaction between certain photodegraded chromophores and repeating ester groups aids in the recovery of the chromophores. Such evidence helps to further uncover the mechanisms responsible for self-healing phenomena observed in some photodegraded dye-doped polymers at the molecular scale.

2 Self-Healing Experiment

The chromophore used in this study was R6g perchlorate, purchased from Sigma-Aldrich. The dye was doped in poly(tetramethylene glycol)-based thermoplastic polyurethane (TPU), glycol-modified poly(ethylene terephthalate) co-polymer (PETG), and $>98\%$ hydrolyzed poly(vinyl alcohol) (PVOH) matrices. The chemical structures of the dye and polymers are shown in Fig. 1. The Fourier-transform infrared (FTIR) spectra for the clean polymers TPU, PETG, and PVOH, without any dopants, are shown in Fig. 1. The FTIR spectra of both undoped TPU and undoped PETG have two similar sets of absorption regions outside of the fingerprint region. The broad set of peaks at $\sim 2900\,\text{cm}^{-1}$ is characteristic of the carbon hydrogen bonds in the polymers. The peaks observed at $1726\,\text{cm}^{-1}$ in TPU and $1713\,\text{cm}^{-1}$ in PETG are due to a carbonyl group vibration, where the lines are pulled due to the presence of carbonyl group being present in either the urethane (TPU) or ester (PETG) functional groups. The FTIR spectrum of undoped PVOH has two prominent sets of absorption regions outside of the fingerprint region; the first being a broad absorption band at $\sim 3250\,\text{cm}^{-1}$ which is characteristic of alcohols, and a second set of peaks surrounding $\sim 2900\,\text{cm}^{-1}$ caused by the carbon-hydrogen bonds in the polymer. A small amount of absorption is observed at $1730\,\text{cm}^{-1}$ and at slightly shorter wavelengths due to some carbonyl oscillations, consistent with

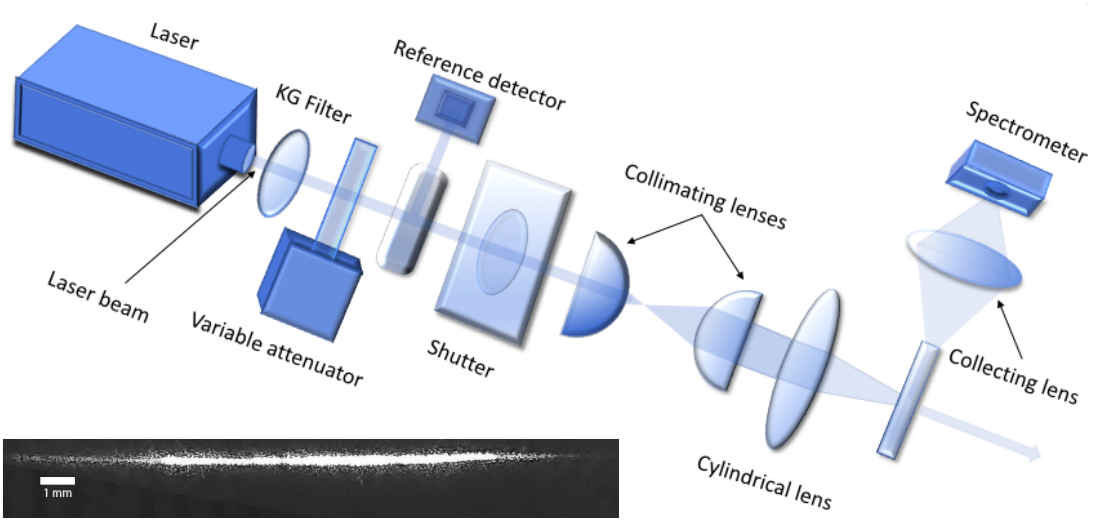

Fig. 2 The setup for the dual photodegradation and recovery experiment. The beam profile is shown below the diagram.

a small concentration of acetate functional groups in 98% hydrolyzed PVOH. The ends of the PVOH chains are also expected to be terminated with an aldehyde group.

The TPU was obtained from Lubrizol as the brand name Pellethane 2363-80A, the PETG was purchased from 3DXTech under the brand name 3DXMAX PETG, and the PVOH was purchased from Sigma-Aldrich. We dissolved TPU in tetrahydrofuran at a ratio of 1:15, PETG in chloroform at a ratio of 1:10, and PVOH in $>18\text{M}\Omega$ deionized water at a ratio of 1:15. The polymer pellets dispersed in solvents where capped in glass bottles and sealed with Parafilm. The TPU and PETG dissolved within two hours in a bath sonicator. The PVOH solution needed to be repeatedly heated to $>90\,^{\circ}\text{C}$, shaken, and sonicated for several hours until fully dissolved. R6g was dissolved in the solution at a nominal 1 wt.% with respect to the mass of the dissolved polymer.

Thin polymer films were fabricated by spin coating the solutions onto 1"×1" glass substrates. The solutions where extracted from their bottles and enough solution was dispensed onto a glass substrate to completely cover a single side. The spin speed was between 500 rpm and 800 rpm depending on the viscosity of the solution. The newly made samples were allowed to dry for a minimum of 15 minutes and then annealed at 120 °C for 20 minutes.

A Continuum Surelite II, Nd:YAG laser was used to both photodegrade the samples and probe the ASE as a function of time. The laser pulse widths were approximately 6ns FWHM with a 10 Hz repetition rate. The 1064 nm fundamental was frequency doubled to operate at a wavelength of 532 nm. The laser power was maximized by optimizing the Q-switch delay, which also led to an increase in the shot-to-shot stability after all transient temperature behavior had left the system. The laser was allowed to reach a static temperature by operating for 1 hour prior to beginning any photodegradation experiment. The high energy per pulse, required for the best stability of the fundamental mode, was greatly reduced prior to being incident on the sample. The pulse energy was initially reduced by two different reflections from glass substrates at high angles with the reflected beams directed into absorbing beam dumps. The pump beam then passed through a KG-1 filter followed by a 2 O.D. neutral density filter.

The pump beam continued through a variable attenuator mounted onto a linear actuator. The beam was then split by another glass substrate. The reflected beam was incident upon an Ophir PE-10C pyroelectric detector. The detector signaled to an Ophir Juno USB power meter that was interfaced with a computer via the manufacturers COM object commands. The reference beam was averaged over 60 pulses (6 seconds) and the variable attenuator was scripted to automatically adjust to any drift slower than the referencing and actuation time. The attenuator was actuated to correct for pump drift when the 60-pulse-average reference energy drifted beyond a $\pm 1.2\%$ threshold relative to the energy referenced at the beginning of the experiment. The actuator was controlled by an Arduino Uno combined with a ZYLtech CNC shield.

The stabilized pump beam was passed through a shutter followed by a 1 O.D. neutral density filter to further reduce the power. When the shutter opened, the beam was expanded with collimating lenses. After the beam was expanded, it passed through a cylindrical lens focused onto a R6G-doped polymer sample. The pump beam's electric-field polarization was oriented perpendicular to the long axis of the beam spot. The pump energy incident on the sample was typically between $\sim 15\,\mu$J/pulse and $20\,\mu$J/pulse at the beginning of every experiment, and stabilized throughout each experiment. The exact pump energy used within this range depended on the threshold at which ASE began to dominate the detected emission over the fluorescence signal. The ASE output intensity is very sensitive to small changes in chromophore concentration when pumping just above the ASE threshold intensity (the pump intensity required to acquire an ASE signal which dominates the fluorescence).

The ASE signal was captured by a lens focused onto the end of a $600\,\mu$m diameter multimode optical fiber which fed into an Ocean Optics USB 4000 spectrometer. The spectrometer was interfaced with a computer using the open source Seabreeze pack-

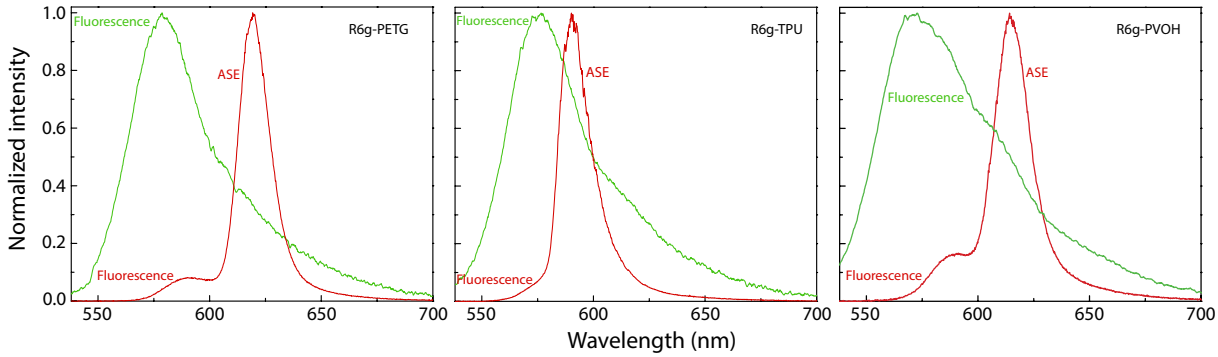

Fig. 3 The normalized fluorescence and ASE spectra for the respective 1 wt.% R6g doped PETG, TPU, and PVOH polymer matrices.

age in Python. A diagram of the relevant optical components in the experiment are shown in Fig. 2. The beam profile, incident on the sample and imaged onto a Sony IMX258 CMOS sensor, is shown beneath the experiment diagram in Fig. 2.

The experiment consisted of two stages. The first stage measured the change in the ASE while the sample was being repetatively pumped at 10 Hz. After the ASE intensity was photodegraded, the shutter was closed. The shutter was actuated by a Denkovi USB relay. The sample was then left in the dark during the second stage of the experiment. While in the dark, the shutter was opened for short durations to probe for signs of recovery via the ASE output intensity. The pump energy referencing/stabilization, shutter control, and ASE spectra collection were integrated into a single Python program for a completely automated photodegradation/recovery experiment.

3 Results

Once excited, the R6g molecules quickly fluoresce, where the excited state lifetimes are less than 1 ns for the high concentrations used in this study.[40,41] The enlongated beam shape, with the long axis perpendicular to the polarization, produced a dominant ASE signal at low pulse energies as compared to a circular beam spot. The ASE peak was red shifted relative to the peak fluorescence, as expected. The degree of red shift in the ASE peak relative to the fluorescence peak depended on the host polymer (shown in Fig. 3). The smallest red shift occurred in TPU while R6g-PVOH had the largest observed red shift. The fluorescence spectrum was also much broader in PVOH as compared to the other two polymer hosts. Inhomogeneous broadening of both the fluorescence and ASE spectra was observed due to the microscopic, heterogenous, polymer environment. An interesting feature of the ASE spectrum of R6g-TPU is the significant asymmetry, which is remarkably similar to the fluorescence. The TPU matrix gave the largest R6g ASE output intensity for a given pump intensity above threshold despite the cloudiness of the TPU host. The R6g-TPU samples also showed the greatest peak fluorescence relative to the other two materials under the same pumping conditions while collecting the spectra shown in Fig. 3. Although there was a significant amount of scattering in the cloudy TPU matrix, which corresponds to losses along the ASE strip, the highly fluorescent R6g-doped TPU system resulted in a low ASE threshold.

The ASE degradation and recovery spectra for a thin film of R6g-doped PETG is shown in Fig. 4(a) and the transient recovery of a typical R6g-PETG sample is shown in Fig. 4(b). To the authors' knowledge, this is the *first report* of a photodegraded chromophore recovering in a polyethylene terephthalate-based polymer. The approximate integrated ASE power was determined by a multi-peak Gaussian fit. The recovery of photodegraded R6g is hypothesized to be mediated by the repeating ester groups in the polymer backbone. For polymers with high concentrations of repeating ester groups and low percentage of photodegraded dopant chromophores, we assume a simple rate equation with a linear dependence on the number of chromophores. The exponential growth solution of the rate equation describing the chromophore recovery is given by

$$\frac{c(t)}{c_0} = 1 - \frac{c_0 - c_{\mathrm{sh}}}{c_0} e^{-(t-t_{\mathrm{sh}})/\tau}, \tag{1}$$

where c_0 is the concentration of R6g in the pristine sample, c_{sh} is the concentration of R6g immediately after the shutter is closed, t_{sh} is the time that the shutter closed, and τ is the recovery time constant.

A simple linear relationship between the concentration of emitters and ASE output intensity can be assumed for small changes in the ASE intensity when just above the threshold concentration, c_{thresh}. For a constant and uniform pump intensity,

$$\frac{I}{I_0} \approx K \frac{c(t) - c_{\mathrm{thresh}}}{c_0}, \tag{2}$$

where I_0 is the ASE output intensity of the pristine sample and K is a constant of proportionality. Provided that the increase in the net intensity is small, a greater than unity recovery of the ASE output intensity can be introduced through the proportionality constant K. The proportionality constant does not describe a specific mechanism causing the surplus, whether it be caused by annealing, increased quantum yield, or another mechanism. Combining Eqs. 1 and 2, the normalized ASE output intensity can be fit by an equation of the form

$$y(t) = A - Be^{-(t-t_{\mathrm{sh}})/\tau}, \tag{3}$$

where A and B are related to the parameters K, c_0, c_{sh}, and c_{thresh}.

The recovery time constant for the sample with a recovery curve shown in Fig 4(b) was (209 ± 16) minutes. There was a

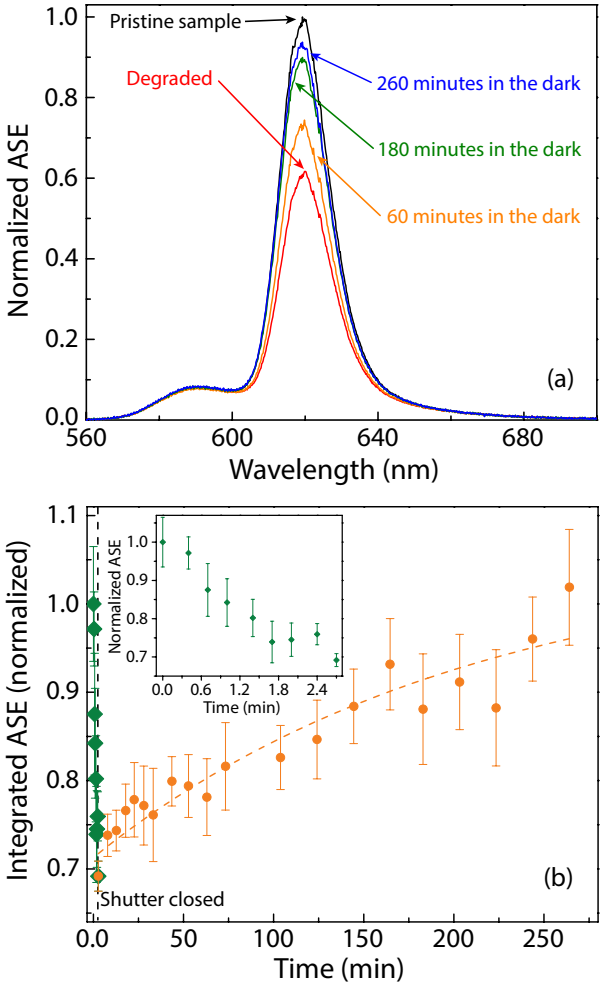

Fig. 4 (a) ASE spectrum of an R6g-PETG sample. (b) The integrated ASE during the degradation (diamonds) and recovery (circles) experiments. The dashed vertical line indicates the last data collected during the degradation experiment. The photodegradation data is shown in the inset.

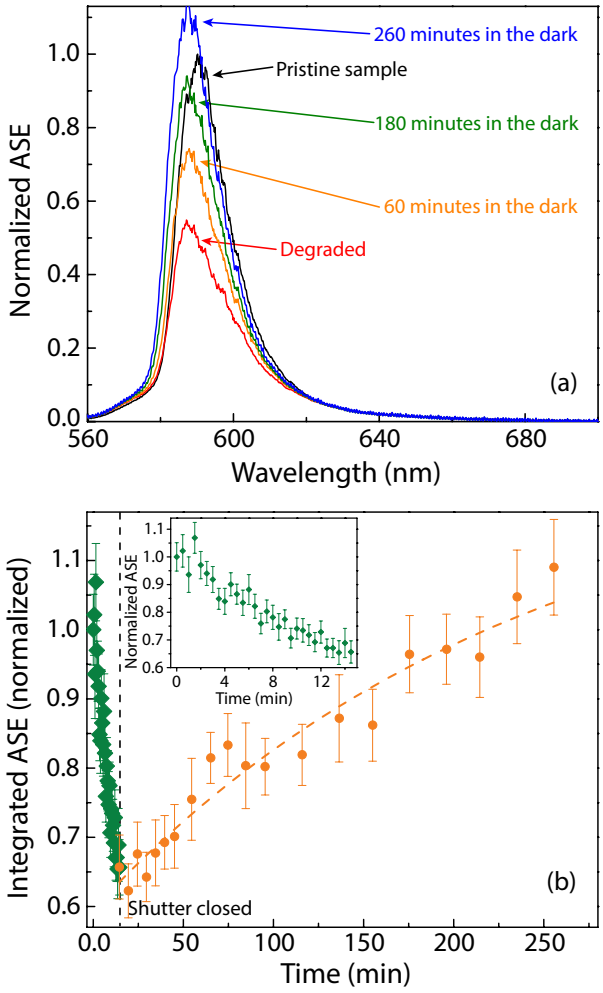

Fig. 5 (a) ASE spectrum of an R6g-TPU sample that shows recovery beyond 100% with respect to the pristine sample. (b) The transient behavior of the ASE during photodegradation and recovery. The photodegradation data is shown in the inset.

small blue shift observed in the fully recovered ASE spectrum of the R6g-PETG system relative to the ASE spectrum obtained from the pristine sample. The blue shift was measured to be (2 ± 1) Å.

The ASE spectrum for the pristine, photodegraded, and recovered states of a R6g-doped TPU thin film is shown in Fig. 5(a). The TPU polymer is a heterogeneous light scatterer with very poor optical clarity when compared to the transparent PETG and PVOH films. There were significant differences in the degree of cloudiness visible to the naked eye between each spin coated film of R6g-doped TPU. The best films were obtained by trapping the solvent vapors via spin coating under a small container that was turned upside-down over the sample. The solvent was allowed to rest under the container and continue to evaporate with the vapors escaping around the bottom of the container after the rotation had finished.

The R6g-doped TPU transient recovery curve is shown in Fig. 5(b). There are three main differences between the R6g-PETG and R6g-TPU transient recovery curves. The first difference is the significant increase in the fully recovered ASE output intensity in the R6g-TPU films over the R6g-PETG films. A recovery of greater than 100% has been previously reported in R6g-polyurethane lasers[37] and in ASE measurements of disperse orange 11 (DO11)-doped polylactic acid (PLA).[39] Because both TPU and PLA have poor optical clarity relative to acrylic, irreversible laser-induced annealing from the pump beam are likely responsible for the large increases observed in their ASE output intensities after the population of chromophores has recovered.

The second difference between the R6g-doped PETG and TPU polymers was the time-dependence of the ASE signal's recovery. The ASE output intensity during recovery deviates from the simple exponential growth of the concentration. A non-exponential growth could be caused by the ester groups in the copolymer being too low; however, the difference in the time dependence between R6g doped in the clear PETG polymer versus the cloudy TPU is likely caused by a change in the effective strip length. We assumed a simple model for the ASE output intensity's dependence on the average dye concentration in a cloudy material by allowing the effective strip length to change with concentration. Note that a heterogenous matrix should also have a het-

erogeneous distribution of the local gain and spontaneous emission cross-sections; however, we assume that these parameters are slowly varying and are approximated as constant in our simplified model. If the sample is being pumped just above threshold where the ASE intensity begins to dominate the fluorescence output, then small sections of the strip length can drop below the ASE dominance threshold when the population of emitters decreases in the matrix. The resultant simplified model of ASE in cloudy materials assumes a reduction in the 'effective' strip length with respect to a heterogeneous decrease in the concentration. Note that the pump beam profile is assumed uniform, but possible hot spots in the incident pump beam profile and the gradients associated with the pump beam's eccentric shape can also cause the non-exponential-like growth in some ASE recovery experiments, where a significant change in the effect strip length can occur in such cases.

A simple lumped-sum model in the form of Shaklee and Leheny[42] may be written for the ASE intensity as a function of an effective strip length,

$$I = I_{\text{pump}} \frac{J}{g} \left(e^{g l_{\text{eff}}} - 1 \right), \tag{4}$$

where J relates to the spontaneous emission cross-section, g is the net gain (gain minus the loss) averaged over the ASE spectrum, I_{pump} is the average pump intensity over the ASE strip, and l_{eff} is the effective length of the ASE strip. We still assume that the spontaneous emission cross-section just above threshold has an approximate linear dependence with the concentration for small changes in the R6g concentration, i.e., $\Delta J \propto \Delta c / c_0$ for $\Delta c \ll c_0$. The effective strip length can also be approximated as a linear function of the concentration for small changes,

$$l_{\text{eff}} \approx l_0 + b \left(\frac{c}{c_0} - 1 \right), \tag{5}$$

where l_0 is the effective length of the ASE strip for the pristine sample's concentration and b is the slope of the straight line. Substituting Eq. 1 and Eq. 5 into Eq. 4 gives the functional form for the time-dependent recovery of the normalized ASE intensity from the R6g-TPU sample,

$$y_{\text{eff}}(t) = A \left(1 - B e^{-(t - t_{\text{sh}})/\tau} \right) \left\{ \exp \left[a \left(1 - B e^{-(t - t_{\text{sh}})/\tau} \right) \right] - 1 \right\} - D, \tag{6}$$

where A translates the concentration dependence to the ASE intensity above threshold, B depends on both c_0 and c_{sh}, $C = \exp[g(l_0 - b)]$, $a = gb$, t_{sh} and τ are still the respective shutter closure time and recovery time constant, and D is associated with the threshold concentration. Note that the gain can also be made concentration dependent, where a linear approximation can be made similar to that for the effective strip length in Eq. 5. The resultant expression will be similar in form to Eq. 6 provided that the gain is only minimally affected by small changes in concentrations such that the reciprocal of the gain can be approximated as constant. The fit to the R6g-TPU sample's transient recovery is given by the dashed line in Fig 5(b), where the recovery time constant is estimated to be (240 ± 144) minutes. Even after making several approximations and simplifying assumptions, Eq. 6 is still highly parameterized. The large number of parameters heavily influences the uncertainty of the fitted time constant to the recovery data.

The degree of blue shift in the peak ASE output is the third difference between the R6g-doped PETG and TPU films. There is no observable shift in the fluorescence within the spectrometer's precision, where the blue shift in the recovered ASE spectrum is not caused by perturbed energy states. The irreversible changes in the local polymer environment do not appear to perturb the molecular resonances, and therefore we also assume that they have a negligible effect on the dipole transition moments and excited state lifetimes. The observation of a static fluorescence peak reinforces the idea that greater than unity recovery of ASE is caused by microscopic physics changes in the matrix instead of quantum changes in the system. Even a small amount of laser-induced annealing in a cloudy sample can shift the ASE gain envelope to the blue because of the blue shift in the Rayleigh scattering curve. As we see in Fig. 6, a significant blue shift occurs during the photodegradation period. Most of the laser-induced annealing occurs at the center of the ASE strip where the pump intensity is highest; the population of photodegraded chromophores is also highest in the center of the pump beam along the ASE strip. When the shutter is closed and the concentration of emitters begins to increase at the center of the strip, where most of the annealing occurs, a more prominent blue shift is observed in the ASE output intensity. Note that there are other mechanisms that can cause the peak ASE spectrum to shift, but laser-induced annealing is the dominant mechanism in this study. Self-healing of a R6g-doped polyurethane gain medium was previously reported in a random laser, where a net red shift was observed and caused by a completely different mechanism.[37]

Laser-induced annealing reduces the loss at the ASE wavelengths in the TPU matrix. The rapid blue shift is directly related to the rapid increase in the measured ASE output within the first two minutes of the photodegradation experiment. The net gain in Eq. 4 is the gain from the dye molecules minus the loss from light scattering in the TPU host. When the matrix is rapidly annealed, the ASE light quickly becomes less scattered, which results in a "jump" of the ASE output intensity. If the reduction in loss is irreversible and there is little laser-induced annealing that occurs after the first few minutes of the photodegradation experiment in the R6g-TPU sample, then loss due to scattering can be considered constant during the recovery phase of the experiment. The final recovered ASE intensity will, however, be greater than the ASE intensity of the pristine sample due to the irreversible laser-induced annealing. The rapid rise in ASE intensity at the beginning of the experiment and the greater than 100% recovery are shown in Fig. 5. The mechanism responsible for the initial rise in ASE intensity and the dominant mechanism responsible for the observed recovery beyond 100% is attributed laser-induced annealing of the cloudy TPU host.

The uncertainties in the final data points for any given data run and material under investigation were similar, where the uncertainty was primarily sourced from the shot-to-shot noise of the pump fundamental. Although the experiment corrected for drift in the mean pump energy/shot averaged over many seconds, the

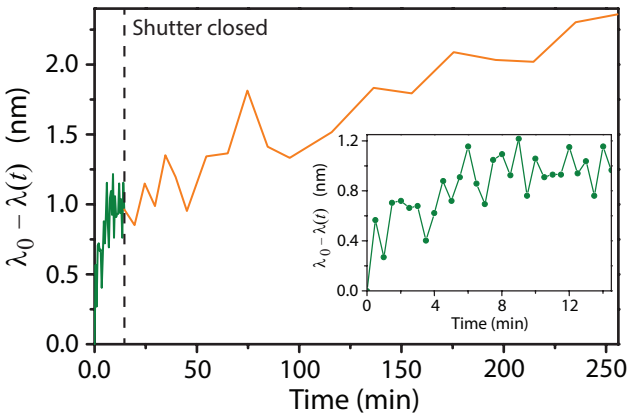

Fig. 6 The difference between the peak ASE wavelength of the pristine R6g-doped TPU sample λ_0 and the peak ASE wavelength at all later times $\lambda\,(t)$ as a function of time. The difference in peak wavelength during the photodegradation stage is shown in the inset.

shot-to-shot noise was inherent to the pump and unavoidable. The mean values for the final data points showed a greater than 100% recovery of the integrated ASE signal for the R6g-doped PETG system, but those mean values were not as high as the final integrated ASE data points obtained in the R6g-doped TPU system. The R6g-doped PETG samples had mean recovery values that were greater than those of the pristine sample values, but the lower limits based on the uncertainty were below 100% recovery. The mean values for the integrated ASE in R6g-doped TPU samples after recovery were always greater than those in pristine samples, and even the lower limits of the recovered values, based on the standard deviation of collected data points, showed a greater than 100% recovery.

The esters in the chemical structure of TPU and PETG are hypothesized to promote the recovery of R6g from a dominant photodegraded state. Other dye-doped polymer systems that have significant self-healing attributes, such as DO11-doped PMMA[43] and PLA[39] have polymer hosts with repeating ester groups. It is interesting to note that the R6g molecule contains an ester in its structure, where recovery could possibly be induced by neighboring molecules. Quenching of the fluorescence is also attributed to aggregates of the R6g chromophore which would likely leave such recoveries undetected in ASE measurements.

The photodegradation and recovery of the ASE spectrum for a R6g-PVOH sample is shown in Fig. 7(a). There is a rapid recovery of R6g in PVOH between the last photodegradation measurement and the first recovery measurement shown in Fig. 7(b). The sample was left in the dark for 2 minutes after the last photodegradation measurement and before the first recovery measurement. Reversal of R6g from an *a priori* dark state with a longer-lifetime than a triplet excited state lifetime was previously reported in PVOH,[44] which accounts for the initial jump in the integrated ASE signal. A similar jump is observed in Fig. 4(b) for an R6g-doped PETG sample. There appears to be some initially long-time-scale recovery in Fig. 7(b) followed by further photodegradation of the signal over time. The PVOH matrix was significantly hydrolyzed, but approximately 2% of the polymer's side groups are acetate groups instead of hydroxyl groups. The acetate functional group

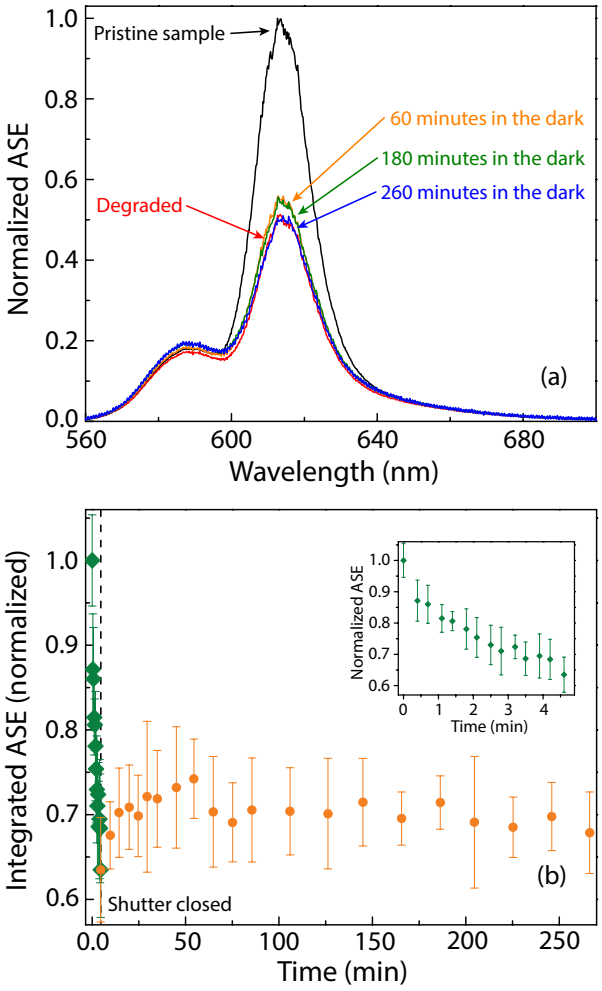

Fig. 7 (a) ASE spectrum and (b) transient ASE signal of a R6g-PVOH sample showing an small initial recovery while in the dark followed by further photodegradation caused by probing. The photodegradation data is shown in the inset.

could possibly promote R6g recovery in a polymer matrix, where a fraction of the photodegraded dye molecules would recover to their pristine state. The continued photodegradation of the ASE intensity at long-time scales is attributed to the periodic probing of the sample to record the ASE intensity during the recovery stage of the experiment.

Ramini et al. showed that classical particle diffusion was not responsible for the observed recovery of the DO11-doped PMMA system's emissive properties,[45] where the behavior of the photobleached profile during recovery is quite different than the behavior predicted with diffusion models. The R6g molecule's long axis is larger than the long axis of DO11. Approximating both molecules as spheres with radii to be one-half the diameter of the long axis, the Stokes-Einstein relation gives a smaller diffusion coefficient for R6g relative to DO11 in environments with the same local viscosities. The three polymer matrices used in this study were all thermoplastic polymers, two of which were studied well below their glass transition temperatures (PETG, $\sim 80^\circ$ C; PVOH, $\sim 80^\circ$ C), where the local viscosity was assumed to be quite large in both materials. The TPU matrix had the least hardness

of the polymers in this study, and its glass transition temperature, $\sim(-40^\circ\,\mathrm{C})$, is below room temperature; however, the polymer at room temperature is still well below its Vicat softening temperature of $\sim 85^\circ\,\mathrm{C}$. The partial healing of R6g observed in the PVOH matrix opposes classical diffusion models, which should follow basic particle diffusion principles and asymptotically reach a uniform steady-state distribution relative to the bulk sample. From previous and current observations, we conclude that the mechanisms of self-healing in all systems being reported in this paper are predominantly chemical in nature and not attributed to long-range mass transport.

Both PETG and TPU contain repeating ester units in their backbones, and R6g was observed to recover from a photodegraded state in both matrices. A small amount of recovery was observed in the PVOH matrix, which has sparsely dispersed acetate groups and residual aldehydes. The formation and reversal of R6g from an *a priori* dark state was also reported for R6g-doped PVOH,[44] albeit on a relatively fast time scale, and it is the likely mechanism responsible for the initially large increase in the ASE signal within the first two minutes of the recovery portion of the experiment. Previous reports of self-healing chromophores were also observed in PMMA,[21] PLA,[39] and polyurethane hosts,[37] all of which contain esters in either the backbone or side chains. It would appear that repeating ester units allow for the recovery of some chromophores through a polymer mediated mechanism. If we assume that the DO11-MMA-oxetane formation route proposed by Hung et al.[43] for the DO11-PMMA system is similar to the recovery process of the R6g-TPU and R6g-PETG systems, then a similar reaction with the carbonyl carbon on the ester groups is a likely suspect. Testing for R6g recovery in polyamide and polyimide could help to determine the favorability of this type of process occurring in a broader class of polymers that contain repeating carbonyl groups without the ester oxygen atom. Studying the effects of the R group atom type on the possible reactions with ester groups may also prove useful, where the results of a self-healing study using polycarbonate as the host could provide valuable insights for uncovering intricacies associated with possible recovery pathways.

4 Conclusion

The transient shot-to-shot ASE output intensities were measured for R6g in three different polymers at a 1 wt.% concentration. The ASE power was reduced via photodegradation of the dye molecule. Self-healing was observed in dye-doped R6g-TPU and R6g-PETG systems allowed to rest in the dark. There was a small amount of recovery in $> 98\%$ hydrolyzed PVOH, which was primarily attributed to a small population of R6g chromophores relaxing from a long-lived dark state. A very small amount of long-time-scale recovery of R6g-doped PVOH films is possibly due to interactions with residual acetate functional groups. The recovered ASE signal of R6g in both TPU and PETG was greater than unity with the largest recovered signals observed in R6g-doped TPU. A large spectral line pull of the ASE peak wavelength occurred in R6g-doped TPU, which was attributed to permanent changes in the cloudy polymer matrix via laser-induced annealing.

The TPU and PETG polymers both contain repeating ester units in the polymer backbone, which are hypothesized to mediate chromophore recovery. Additional experiments using polymers with different repeating functional groups should provide new insights into specific recovery mechanism(s). These experiments and future studies could be used to tailor self-healing materials for specific applications such as organic, solid-state, distributed feedback and distributed Bragg reflector lasers.

Acknowledgments

NJD thanks the Hawaii Pacific University, College of Natural and Computational Sciences, Scholarly Endeavors Program for supporting this work. NJD also thanks the Department of Natural Sciences at Hawaii Pacific University for startup funds that made this study possible. All authors thank Professor David Horgen as well as Pat Allen and the Natural Sciences Laboratories staff at Hawaii Pacific University for assistance with chemical processing and characterization equipment.

Notes and references

1 H. Zollinger, *Color Chemistry: syntheses, properties, and applications of organic dyes and pigments* (VCH, New York, 1987).

2 S. S. Sun and N. S. Sariciftci, *Organic photovoltaics: mechanisms, materials, and devices* (CRC Press, Boca Raton, 2005).

3 Y. Su, S. C. Lan, and K. H. Wei, "Organic photovoltaics," Mater. Today **15**, 554–562 (2012).

4 P. N. Prasad and D. J. Williams, *Introduction to nonlinear optical effects in molecules and polymers* (Wiley, New York, 1991).

5 S. R. Marder, "Organic nonlinear optical materials: where we have been and where we are going," Chem. Commun. **2**, 131–134 (2006).

6 M. S. T. Gonçalves, "Fluorescent labeling of biomolecules with organic probes," Chem. Rev. **109**, 190–212 (2008).

7 S. Luo, E. Zhang, Y. Su, T. Cheng, and C. Shi, "A review of nir dyes in cancer targeting and imaging," Biomaterials **32**, 7127–7138 (2011).

8 M. Yamashita and H. Kashiwagi, "Photodegradation mechanisms in laser dyes: a laser irradiated esr study," IEEE J. Quant. Electron. **12**, 90–95 (1976).

9 S. Sinha, S. Sasikumar, A. K. Ray, and K. Dasgupta, "The effect of dye photodegradation on the performance of dye lasers," Appl. Phys. B **78**, 401–408 (2004).

10 A. N. Fletcher, D. A. Fine, and D. E. Bliss, "Laser dye stability part 1. flash frequency and fluid filtration effects," Appl. Phys. A **12**, 39–44 (1977).

11 A. Kurian, N. A. George, B. Paul, V. P. N. Nampoori, and C. P. G. Vallabhan, "Studies on fluorescence efficiency and photodegradation of rhodamine 6g doped pmma using a dual beam thermal lens technique," Laser Chem. **20**, 99–110 (2002).

12 A. Migani, V. Leyva, F. Feixas, T. Schmierer, P. Gilch, I. Corral, L. Gonzalez, and L. Blancafort, "Ultrafast irreversible phototautomerization of o-nitrobenzaldehyde," Chem. Commun. **47**, 6383–6385 (2011).

13 T. Bernas, E. K. Asem, J. P. Robinson, P. R. Cook, and J. W.

Dobrucki, "Confocal Fluorescence Imaging of Photosensitized DNA Denaturation in Cell Nuclei," Photochem. Photobiol. **81**, 960–969 (2005).

14 H. Ohkita, W. Sakai, A. Tsuchida, and M. Yamamoto, "Charge Recombination of Electron-Cation Pairs Formed in Polymer Solids at 20K through Two-Photon Ionization," J. Phys. Chem. B **101**, 10241–10247 (1997).

15 R. Zondervan, F. Kulzer, M. A. Kolchenko, and M. Orrit, "Photobleaching of Rhodamine 6g in Poly(vinyl alcohol) at the Ensemble and Single-Molecule Levels," J. Phys. Chem. A **108**, 1657–1665 (2004).

16 G. E. Hall and P. L. Houston, "Vector Correlations in Photodissociation Dynamics," Annu. Rev. Phys. Chem. **40**, 375–405 (1989).

17 M. Mac, J. Najbar, and J. Wirz, "Fluorescence and intersystem crossing from the twisted intramolecular charge transfer (TICT) state of bianthryl in the presence of inorganic ions in polar solvents," J. Photochem. Photobiol. A **88**, 93–104 (1995).

18 S. K. Ramini and M. G. Kuzyk, "A self healing model based on polymer-mediated chromophore correlations," J. Chem. Phys. **137**, 054705 (2012).

19 W. J. Priest and M. M. Sifain, "Photochemical and thermal isomerization in polymer matrices: Azo compounds in polystyrene," J. Polym. Sci. A **9**, 3161–3168 (1971).

20 G. D. Peng, Z. Xiong, and P. L. Chu, "Fluorescence decay and recovery in organic dye-doped polymer optical fibers," J. Lightwave Technol. **16**, 2365 (1998).

21 B. F. Howell and M. G. Kuzyk, "Amplified spontaneous emission and recoverable photodegradation in polymer doped with Disperse Orange 11," J. Opt. Soc. Am. B **19**, 1790–1793 (2002).

22 N. Tanaka, N. Barashkov, J. Heath, and W. N. Sisk, "Photodegradation of polymer-dispersed perylene di-imide dyes," Appl. Opt. **45**, 3846–3851 (2006).

23 B. Anderson, S.-T. Hung, and M. G. Kuzyk, "Influence of an electric field on photodegradation and self-healing in disperse orange 11 dye-doped pmma thin films," J. Opt. Soc. Am. B **30**, 3193–3201 (2013).

24 B. Anderson and M. G. Kuzyk, "Generalizing the correlated chromophore domain model of reversible photodegradation to include the effects of an applied electric field," Phys. Rev. E **89**, 032601 (2014).

25 S. K. Ramini, B. Anderson, S.-T. Hung, and M. G. Kuzyk, "Experimental tests of a new correlated chromophore domain model of self-healing in a dye-doped polymer," Polym. Chem. **4**, 4948–4954 (2013).

26 B. R. Anderson, S.-T. Hung, and M. G. Kuzyk, "Imaging studies of temperature dependent photodegradation and self-healing in disperse orange 11 dye-doped polymers," J. Chem. Phys. **145**, 024901 (2016).

27 N. B. Embaye, S. K. Ramini, and M. G. Kuzyk, "Mechanisms of reversible photodegradation in disperse orange 11 dye doped in pmma polymer," J. Chem. Phys. **129**, 054504 (2008).

28 B. R. Anderson, S.-T. Hung, and M. G. Kuzyk, "Wavelength dependence of reversible photodegradation of disperse orange 11 dye-doped pmma thin films," J. Opt. Soc. Am. B **32**, 1043–1049 (2015).

29 B. Anderson, S.-T. Hung, and M. G. Kuzyk, "The effect of pump depletion on reversible photodegradation," Opt. Commun. **318**, 180–185 (2014).

30 B. Anderson, S. K. Ramini, and M. G. Kuzyk, "Imaging studies of photodamage and self-healing in disperse orange 11 dye-doped PMMA," J. Opt. Soc. Am. B **28**, 528–532 (2011).

31 S.-T. Hung, S. K. Ramini, D. G. Wyrick, K. Clays, and M. G. Kuzyk, "The role of the polymer host on reversible photodegradation in disperse orange 11 dye," in "Proc. SPIE," (2012), p. 84741A.

32 Y. Zhu, J. Zhou, and M. G. Kuzyk, "Two-photon fluorescence measurements of reversible photodegradation in a dye-doped polymer," Opt. Lett. **32**, 958–960 (2007).

33 P. Kobrin, R. Fisher, and A. Gurrola, "Reversible photodegradation of organic light-emitting diodes," Applied Physics Letters **85**, 2385–2387 (2004).

34 W. Nie, J.-C. Blancon, A. J. Neukirch, K. Appavoo, H. Tsai, M. Chhowalla, M. A. Alam, M. Y. Sfeir, C. Katan, J. Even, S. Tretiak, J. J. Crochet, G. Gupta, and A. D. Mohite, "Light-activated photocurrent degradation and self-healing in perovskite solar cells," Nature communications **7**, 11574 (2016).

35 P. Dhakal and M. G. Kuzyk, "Molecular structure and reversible photodegradation in anthraquinone dyes," J. Photochem. and Photobiol. A **328**, 66–76 (2016).

36 B. R. Anderson, R. Gunawidjaja, and H. Eilers, "Self-healing organic-dye-based random lasers," Opt. Lett. **40**, 577–580 (2015).

37 B. R. Anderson, R. Gunawidjaja, and H. Eilers, "Photodegradation and self-healing in a rhodamine 6g dye and y_2o_3 nanoparticle-doped polyurethane random laser," Appl. Phys. B **120**, 1–12 (2015).

38 B. R. Anderson, R. Gunawidjaja, and H. Eilers, "Random lasing and reversible photodegradation in disperse orange 11 dye-doped pmma with dispersed zro_2 nanoparticles," J. Opt. **18**, 015403 (2016).

39 N. Stubbs, M. Bridgewater, M. Stubbs, M. Crescimanno, M. G. Kuzyk, and N. J. Dawson, "Polylactic acid promotes healing of photodegraded disperse orange 11 molecules," Opt. Mater. **76**, 11–15 (2018).

40 M. Fedoseeva, R. Letrun, and E. Vauthey, "Excited-State Dynamics of Rhodamine 6G in Aqueous Solution and at the Dodecane/Water Interface," J. Phys. Chem. B **118**, 5184–5193 (2014).

41 J. H. Andrews, M. Crescimanno, N. J. Dawson, G. Mao, J. B. Petrus, K. D. Singer, E. Baer, and H. Song, "Folding flexible co-extruded all-polymer multilayer distributed feedback films to control lasing," Opt. Express **20**, 15580–15588 (2012).

42 K. L. Shaklee and R. F. Leheny, "Direct determination of optical gain in semiconductor crystals," Appl. Phys. Lett. **18**, 475–477 (1971).

43 S.-T. Hung, A. Bhuyan, K. Schademan, J. Steverlynck, M. D.

McCluskey, G. Koeckelberghs, K. Clays, and M. G. Kuzyk, "Spectroscopic studies of the mechanism of reversible photodegradation of 1-substituted aminoanthraquinone-doped polymers," J. Chem. Phys. **144**, 114902 (2016).

44 R. Zondervan, F. Kulzer, S. B. Orlinskii, and M. Orrit, "Photoblinking of Rhodamine 6G in Poly(vinyl alchohol): Radical Dark State Formed through the Triplet," J. Phys. Chem. A **107**, 6770–6776 (2003).

45 S. K. Ramini, N. Dawson, and M. G. Kuzyk, "Testing the diffusion hypothesis as a mechanism of self-healing in disperse orange 11 doped in poly(methyl methacrylate)," J. Opt. Soc. Am. B **28**, 2408–2412 (2011).